THE EFFECT OF PIPE-LINE STRUCTURE ON THE FLAMMABILITY CHARACTERISTICS OF HYDROGEN-AIR PREMIXED GAS UNDER END-OPENING CONDITIONS

by

Ning ZHOU [a], ***Xi CHEN*** [a], ***Xue LI*** [a*], ***Bing CHEN*** [b], ***Ying ZHANG*** [a], ***Weibo HUANG*** [a], ***Xuanya LIU*** [c], ***Jiawei TIAN*** [a], ***Yongbin YU*** [a], ***Tianxiang SUN*** [a], ***Weiqiu HUANG*** [a], ***Chunhai YANG*** [d], ***and Huijun ZHAO*** [a]

[a] School of Petroleum Engineering, Changzhou University, Changzhou, China
[b] Institute of Industrial Safety, China Academy of Safety Production Research, Beijing, China
[c] Tianjin Fire Research Institute of MEM, Tianjin, China
[d] School of Materials Engineering, Changshu Institute of Technology, Suzhou, China

Original scientific paper
https://doi.org/10.2298/TSCI220910191Z

The pipe structures and opening conditions have an important influence on gas explosion, but little research has been done on the coupling analysis of the two. In order to reveal the effect of pipe structure on the flammability characteristics of hydrogen-air premixed gas under end-opening conditions, the flame structure, flame propagation velocity, explosion pressure and flow field distribution in the explosion process of hydrogen-air premixed gas in different pipe structures were analyzed by numerical simulation. The results show that the flame propagation velocity and pressure are less influenced by the end-opening structure in the initial ignition stage, however, when the flame propagates to the pipe end, the flame propagation velocity in each pipe structure is significantly enhanced. The 90° elbow has a certain inhibitory effect on the flame development, while the T-shaped bifurcation structure can effectively increase the degree of gas detonation. In pipe with large aspect ratio, due to the wall effect, the effect of acoustic oscillation disturbance on the flame front and the air-flow release effect of the end-opening, there are two peaks and two troughs in the pressure rise rate curve of each pipe-line structure.

Key words*: pipe-line structure, hydrogen-air premixed gas, flame propagation, explosion overpressures, flow field*

Introduction

Hydrogen, as a clean energy, is widely concerned due to its low energy level and wide range of combustibility during ignition [1]. Pipe-line transportation is the main mode of hydrogen transportation. However, due to the special physical and chemical properties of hydrogen, carbon steel is prone to hydrogen embrittlement, and leakage and deflagration accidents are extremely easy to occur during transportation, causing great damage to pipe-lines and surrounding facilities [2-4]. Therefore, sufficient attention should be given to the issue of safe storage and transportation of hydrogen.

Scholars in China and overseas have carried out a series of studies on explosion propagation characteristics and flame propagation dynamics of hydrogen-air premixed gas in

[*] Corresponding author, e-mail: lix@cczu.edu.cn

pipe-lines. In terms of pipe opening conditions, Yu *et al.* [5] conducted an experimental study on the propagation acceleration of hydrogen-air premixed flame in a end-opening pipe. The results show that the propagation state of the flame changes with the change of the hydrogen equivalence ratio. Wen *et al.* [6] analyzed the influence of obstacles in the end-opening pipe on the combustion characteristics of hydrogen-air mixture. The results showed that obstacles promoted the acceleration of hydrogen flame in the experimental pipe section. In terms of pipe structure, Uchida *et al.* [7] studied the influence of explosion wave on the internal pressure of pipe-line in 90° elbow, and the results determined that the pressure load of elbow in two positions was greater than that of straight pipe. One is the peak pressure at the outer edge of the bend due to compression. The other is the second pressure peak caused by shear wave propagation downstream of the elbow outlet. Li *et al.* [8] studied the premixed gas explosion process in a 90° elbow, and the results showed that the elbow structure has an influence on the flame structure in the explosion process. Frolov *et al.* [9] studied the influence of the *U*-shaped pipe structure on the combustion wave and reaction excitation in the pipe, and found that the *U*-shaped elbow promoted the generation of excitation wave, but when the flame propagated through the elbow, the combustion wave in the pipe attenuated. Zhou *et al.* [10-12] carried out experimental and numerical studies on the combustion and explosion characteristics of hydrogen-air premixed gas in confined straight pipe and elbow under different equivalence ratios, as well as the effects of ignition position (horizontal and vertical) and hydrogen addition on the combustion and explosion characteristics of premixed gas in a *T*-shaped bifurcation pipe. The results showed that the maximum flame speed of most combustible premixed gases usually occurs when the equivalence ratio is near 1. While hydrogen-air premixed gas is affected by Graham's law in chemical reaction kinetics, the maximum flame speed occurs near 1.5 times the equivalent ratio. the variation of flame propagation velocity and pressure with pipe length was almost the same at different ignition positions, but the magnitude and position of the pressure, the flame structure and the flow field were different. The addition of hydrogen had an obvious effect on the explosion characteristics of the mixed gas. When the volume fraction of hydrogen exceeded 10%, the strengthening effect of *T*-shaped bifurcation structure on explosion reaction was more significant.

According to previous studies, scholars in China and overseas mostly focus on the influence of single factors such as equivalence ratio, ignition position and obstacles on flame propagation characteristics of single pipe structure, while the research on combustion and explosion in pipes with complex structure and large length diameter ratio is in a minority. However, in addition straight pipes, elbows and *T*-shaped pipes are also the most common forms in pipe-line transportation systems. The wide application of tee, elbow, valve and other non-straight components in industry also leads to the existence of many special pipe structures in the pipe network. According to the current research results on pipes with complex structures, both 90° elbows and *T*-shaped structures in closed pipes can improve the explosion intensity, but there are few research results on open pipes, and even fewer studies on the coupling analysis of gas cloud explosion reaction under the joint action of end openings, elbows and *T*-shaped structures. In industrial sites, the end-opening pipes with external ignition sources are more prone to accidental explosion than fully enclosed pipes, such as large area pipe damage due to external force impact or weathering. As an important geometric feature, the opening condition of the pipe also plays an important role in flame propagation [13, 14]. Therefore, the detonation characteristics of hydrogen air premixed gas in straight pipe, 90° elbow pipe and *T*-shaped bifurcated pipe under end-opening conditions were systematically studied by numerical simulation. The changes of flame structure, flame propagation velocity, flow field and pressure in different pipe structures are analyzed by coupling. The research conclusion will reveal the flame propagation mechanism in the combustion process of hydrogen air premixed gas, and provide a theoretical basis for accident mitigation in the future.

Numerical model and verification

Previous studies of combustion processes have shown that the turbulence model has a sufficient level of accuracy [15], which determined the choice of this model.

Numerical model

The explosion of premixed gas in a confined space is a complex combustion chemical reaction process with strong turbulent flow, and the strong coupling between the flame front and turbulent gas-flow contributes to the complex and changeable flame structure [16]. Therefore, the LES model with Zimont sub-grid model in C equation is applied to reflect the premixed flame reaction progress variables, C is a scalar representing the reaction process:

$$C = \frac{\sum_{i=1}^{n} Y_i}{\sum_{i=1}^{n} Y_{i,e}} \tag{1}$$

Since the effects of 3-D pipe geometry and different flame disturbance factors on flame acceleration are taken into account in LES model, the simulation results of fingertip flame, tulip flame and deformed tulip flame are closer to the experimental results [17, 18]. This model is suitable for complex strong pulsating turbulence, which can more clearly reflect the variation characteristics of flame structure and flow field during combustion, especially for the simulation of flame propagation in confined space [18-20]. The specific equations:

$$\frac{\partial \bar{\rho}}{\partial t} + \frac{\partial \left(\bar{\rho} \tilde{u}_i \right)}{\partial x_i} = 0 \tag{2}$$

$$\frac{\partial \left(\bar{\rho} \tilde{u}_i \right)}{\partial t} + \frac{\partial \left(\bar{\rho} \tilde{u}_i \tilde{u}_j + \bar{p} \delta_{ij} - \tilde{\tau}_{ij} + \tau_{ij}^{sgs} \right)}{\partial x_j} = 0 \tag{3}$$

$$\frac{\partial \rho \tilde{h}_s}{\partial t} + \frac{\partial \rho \tilde{u}_i \tilde{h}_s}{\partial x_i} - \frac{\partial \bar{p}}{\partial t} - \bar{u}_j \frac{\partial \bar{p}}{\partial x_i} - \frac{\partial}{\partial x_i} \left(\lambda \frac{\partial \tilde{T}}{\partial x_i} \right) = -\frac{\partial}{\partial x_j} \left[\rho \left(\tilde{u}_i \tilde{h}_s - \tilde{u}_i - \tilde{h}_s \right) \right] \tag{4}$$

By solving the transport equation of the density-weighted average reaction process variables, the flame front propagation is modeled, and the RANS equation of the reaction process variables averaged by the Favre filter:

$$\frac{\partial}{\partial t}(\bar{\rho}\tilde{c}) + \nabla(\bar{\rho}\tilde{v}\tilde{c}) = \nabla\left(\frac{\mu_t}{\mathrm{Sc}_t}\nabla\tilde{c}\right) + \bar{S}_c \tag{5}$$

In the formula, Sc_t is taken as 0.7, the expression of $\bar{S}_c$:

$$\bar{S}_c = \bar{\rho}_u S_t \Xi_\Delta \left| \nabla c \right| \tag{6}$$

Numerical details

There are three types of pipe structures are used for 3-D numerical simulation, as shown in fig. 1. They are, respectively straight pipe, 90° elbow pipe and *T*-shaped bifurcation pipe, with a diameter of 125 mm and a total length of 5.5 m. Large eddy simulation and

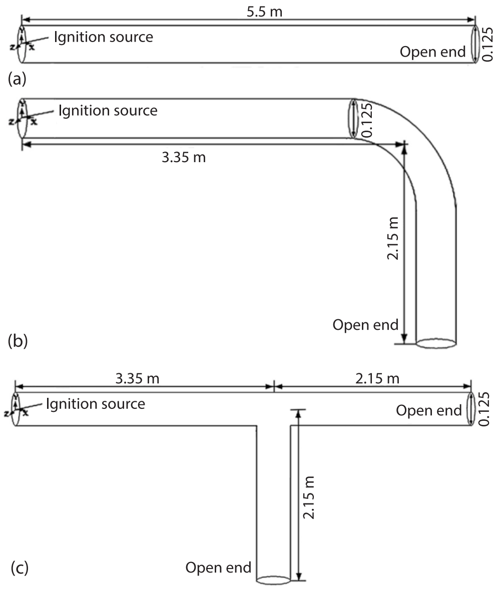

Figure 1. Physical model; (a) the straight pipe, (b) the 90° elbow pipe, and (c) the *T*-shaped bifurcation pipe

Zimont combustion model are adopted, PISO algorithm is selected to couple velocity and pressure, central difference scheme is adopted for diffusion term, and second-order upwind scheme is adopted for convection term. The pipe end is set as the pressure outlet through the boundary conditions, and the rest of the boundary is adopted as the adiabatic wall conditions. The time step is 0.1 ms. The hydrogen-air is fully mixed in the calculation area (equivalence ratio is 1) to form a stable premixed gas at normal temperature and pressure. The laminar flow velocity of the hydrogen-air mixture is set to 2.1 m/s by evaluating with the experimental data which is proposed by Lamoureux [21]. The ignition position is located at the center of the left wall. The ignition energy is 1 J, and the initial temperature and absolute pressure are set at 300 K and 1.0 atm, respectively. The commercial CFD platform FLUENT 16.0 is used to perform the computation.

Mesh independence and model validation

Mesh independence verification

In numerical simulation, the calculation step size and grid size will affect the calculation accuracy. In theory, the smaller the two, the higher the calculation accuracy, but this also increases the calculation cost. Therefore, we should try to balance the calculation cost and accuracy in the process of grid generation. In this paper, the calculation domain of the working condition is the pipe with large length diameter ratio, which is much larger than the ventilation pipe with short diameter ratio. Therefore, considering the calculation cost, four grid sizes (1, 2, 3, 4, 5 mm) are used to analyze and verify the independence of the model. The results are shown in fig. 2. Taking into account the efficiency cost ratio and accuracy, the final calculation grid is 4 mm × 4 mm × 4 mm.

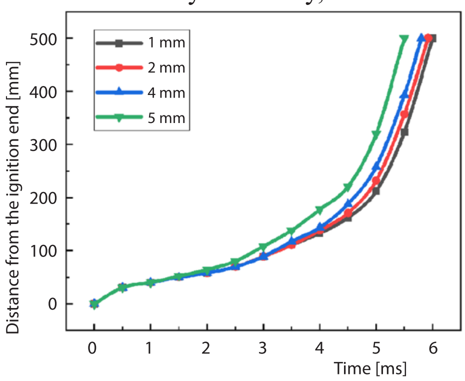

Figure 2. Grid size comparison

Model validation

The physical model is consistent with the explosion experiment system of square tube with obstacles carried out by Lv *et al.* [22]. The cross-sectional dimension of the pipe is 0.1 m × 0.1 m, the length of the pipe is 0.5 m, and the blockage rate is 0.5. The calculated results are shown in fig. 3. In fig. 3(a), the evolution of the flame structure in the numerical simulation is basically consistent with the experimental results, and the time of bifurcation flame is roughly the same (shown by the red solid box). In figs. 3(b) and 3(c), the predicted flame velocity and overpressure by LES are slightly larger than the experimental results. The error of flame velocity and overpressure oscillation frequency between the calculated value and the experimental data is about 7.21%. The main reason is that the cooling effect of the pipe wall is ignored in the numerical simulation process. The predicted flame structure, flame propagation velocity and overpressure are basically consistent with the experimental results, which verifies the reliability of this model. The aforementioned results prove the applicability of LES in the calculation of hydrogen turbulent combustion.

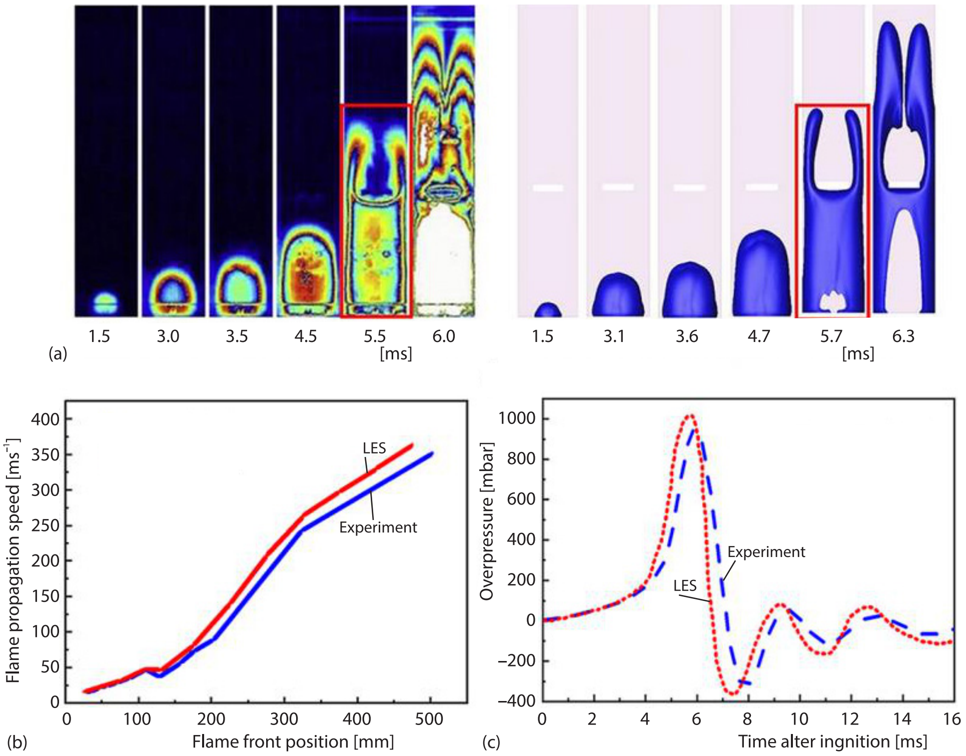

Figure 3. comparison of experimental and simulated results; (a) comparison of flame shapes, (b) comparison of flame propagation speed, and (c) comparison of overpressure

Result and discussion

Flame propagation process and flow field distribution in different pipe-line structures

The flame propagation process is mainly affected by the mixture composition and the interaction between flame propagation and flow field structure [23]. Figures 4-6 show the flame structure and flow field distribution in each pipe structure, and the instantaneous state of flame propagation is reflected by different color. Blue represents the unburned area, red represents the combustion area, and yellow-green represents the flame front. As seen in fig. 4(a), the flame in the straight pipe expands freely at the beginning of ignition and propagates forward in a hemispherical shape. After 4 ms, the flame propagates forward in a fingertip structure restricted by the sidewall surface, and the surface area increases sharply, so the flame accelerates exponentially. When the flame skirt contacts the wall at 7 ms, the surface area quickly lost, resulting in a sharp deceleration of the flame. After that, the flame maintains a stretched fingertip structure and propagates until the pipe end. At 10 ms, fine symmetrical vortexes begin to appear near the ignition end. The gradual development and concentration of vortices lead to the gradual increase of turbulence intensity in the pipe. Higher turbulent kinetic energy accelerates the flame propagation and combustion speed [23]. The farther the flame front is from the ignition end, the more obvious the flame tip stretches, shown in fig. 4(b). The larger the contact area between the unburned gas body and the flame front is, the faster the chemical reaction rate is, and ultimately the flame propagation speed increases.

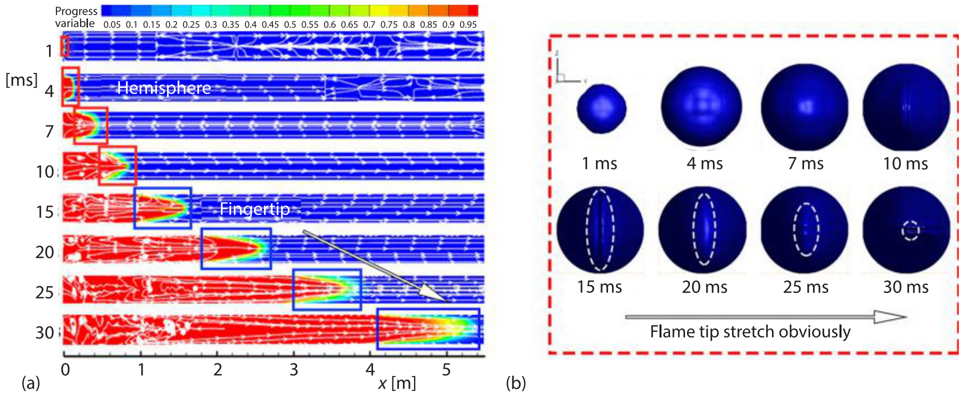

Figure 4. Development process in straight pipe; (a) flame structure and flow field diagram and (b) sectional view

As shown in fig. 5(a), the flame propagation of the premixed flame in the 90° elbow pipe goes through four stages in a end-opening pipe as proposed by Clanet and Searby [24], they are hemispherical flame unaffected by the wall, fingertip flame, flame in contact with the wall, and classical Tulip flame, respectively. The flame propagates in a fingertip structure between 4 ms and 20 ms. The combined effect of the thermal-diffusive instability of hydrogen-air and the shear flow near the wall surface promotes the chemical reaction be accelerated, during which the flame skirt gradually contacts the wall. In 20 ms, the flame structure becomes *flat*. Large-scale vortex clusters are observed near the lower wall of the pipe, and the reverse companion flow appears at the axis position of the burned area (shown by the black dashed box, fig. 5(a). At this time, the flame propagation velocity decreases slightly, as shown in fig. 7. Due to the instability factors such as Darrieus-Landau (D-L) instability and Rayleigh-Taylor (R-T) instability, the *flat* shape of the flame front cannot be maintained [25, 26]. Tulip structure appears at 30 ms, showing a *four-tongue* appearance at z-section, shown by the red dashed box, fig. 5(a). Affected by many factors such as hydrodynamic instability and the interference effect of reflected wave, the vortex flow lines near the flame front, shown by the black solid box, fig. 5(a) are dense, and the range involved is small. The thickness of the flame front is large, which conforms to the characteristics of small-scale strong turbulent flame.

As the combustion proceeds, the flame front reaches the elbow of the pipe-line within 31-32 ms. When the shock wave enters the 90° elbow and propagates along the upper wall, the concentrated reflection of the concave wall structure causes the shock wave to superimpose and form a local high pressure region. In contrast, when the shock wave propagates along the lower wall, the divergent reflection generated by the convex wall structure forces the local pressure to disperse and to form a low pressure region, described in fig. 5(b). The flow field is formed in a specific direction because of the pressure difference, and it isolates the contact between the flame tongue and the unburned gas body to a certain extent, reducing the gas combustion chemical reaction near the concave wall [27]. Finally, the development of the flame tongue and the tendency to fade out at the bend are both obviously inhibited. The flame propagation velocity decreases again. Affected by the tensile effect of rarefaction waves near the lower wall, the outer edge of the lower tongue of the flame is obviously elongated, winding the inner wall, and dominating the flame propagation at the bend, as shown in the partial enlargement, see the black dotted box, fig. 5(a). The flame propagates through the elbow to the end of the pipe within 32-37 ms. Due to the continuous impact of multi-wave systems such as compression wave, rarefaction wave and reflected wave at the elbow, the air-flow in the pipe is disturbed, resulting in an obvious baroclinic effect at the elbow [28], which makes the air-flow in the pipe propagate from the elbow to the pipe ends, respectively. As time increases, the turbulence intensity near the flame front increases and the fold deformation becomes more and more obvious, as seen in the sectional flame structure, shown by the blue dashed box, fig. 5(a), which eventually presents a wedge tip structure, shown by the blue solid box, fig. 5(a). This structure is interpreted as *Squish front* by Xiao *et al.* [17].

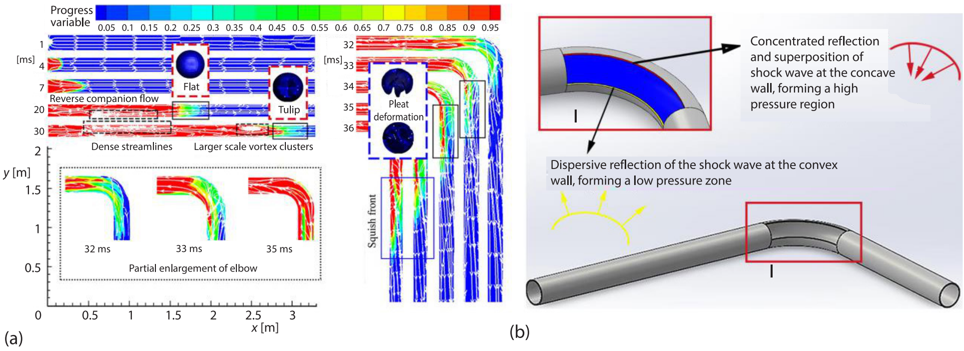

Figure 5. Development process in 90° elbow pipe; (a) flame structure and flow field diagram and (b) schematic diagram of the formation process of the reflected shock wave on the surface of the elbow

Figure 6(a) shows that the premixed flame propagates forward with fingertip structure in a *T*-shaped bifurcation pipe from 2-8 ms, which is similar to the growth pattern of the straight pipe and the 90° elbow pipe, but it takes the shortest time to propagate to 3.35 m. The reason is that the propagation of flame is further promoted by the superposition of the air-flow release effect of the opening structure at both ends. At 15 ms, several small vortex clusters begin to form at the ignition end, and gradually grow larger with the flame propagation, shown by black solid box, fig. 6(a). At this time, the flame structure is still a regular *fingertip* type, its disturbance on the flame structure is weak because the vortex is far from the flame front. About 19 ms, the counterflow begins to appear in the burned area when the flame propagates to the bifurcation. Due to the sudden expansion of the cross-section and the disturbance of the rarefaction and reflected waves near the wall, the flame front begins to destabilize and forms a local turbulent vortex motion, as a result, part of the unburned gas is wrapped in the vortex, as shown in III, IV, fig. 6(a). The development, movement and fragmentation of the vortexs strengthen the combustion reaction. Within 22-24 ms, the flame passes through the bifurcation, during which the combustion rate sharply increases, the flame front folds and deforms, see sectional view, shown in fig. 6(b), and a wedgetip structure appears in the T3 pipe section. This can be explained that the bifurcation is equivalent to the presence of a vent in the lower wall of the horizontal pipe section, which can stimulate the flame propagation when it is located in front of the flametip [29]. As the combustion proceeds, it can be seen that the flame development speed of T3 branch is faster than that of T2 branch, and there is a flame discontinuity in T3 branch pipe, which is caused by the superposition and reflection of the shear wave produced by the collision between the pressure wave at the bifurcation and the wall. Furthermore, a local high pressure is formed, leading to a larger pressure gradient and interfering with the stable development of the flame. The split effect of T3 branch leads to a decrease of flame propagation speed in a short time. The inflection point of the bifurcation wall is equivalent to an obstacle in the flow field, which produces a disturbance and reflection of the air-flow and shock wave. Under the vortex motion, the flame front propagates to the T2 and T3 branch pipes, respectively. The closer the flame to the pipe end, the stronger the traction of the pressure outlet on the flame propagation, and thus the faster the flame propagation speed develops.

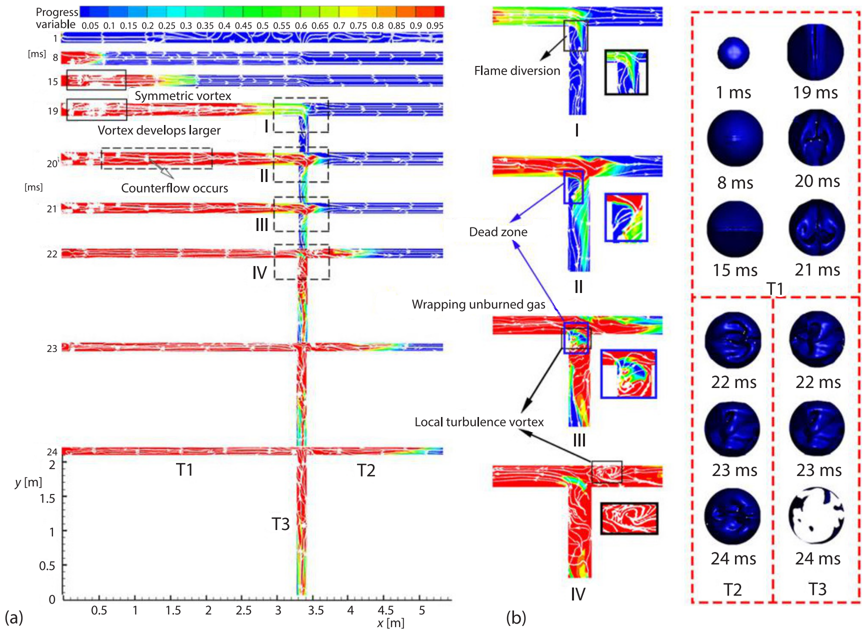

Figure 6. Development process in *T*-shaped bifurcation pipe; (a) flame structure and flow field diagram and (b) pleat deformation of sectional flame surface

Variation law of flame propagation velocity in different pipe-line structures

Figure 7 shows the flame propagation velocities for the open conditions at the end of each pipe structure. It can be observed that in all cases, the oscillation changes of flame propagation velocity in the initial stage (0~2.5 m) are roughly the same, showing a trend of rising first and then falling, and the first peak values of velocity are reached successively in the 1~2 m pipe section, indicating that the earlier flame acceleration mainly relies on the combustion chain reaction of the premixed gas, and the flame propagation process varies less under different pipe structures. Previous studies have shown that the contact between the flame and the pipe wall causes part of the flame to be extinguished at the earlier stage, which weakens the combustion reaction rate of the gas to a certain extent. The aforementioned reasons, along with other factors such as viscous dissipation, lead to the reduction of flame propagation speed after reaching the first peak. When the flame propagates to 2.5 m, the flame propagation velocity changes significantly in different pipe-line structures. The reflected waves generated by the wall restriction of the precursor shock wave in the straight pipe meet the flame front, which increases the turbulent kinetic energy in the pipe and further accelerates the flame propagation. After 2.5 m, under the action of high temperature and high pressure of the precursor shock wave, the unburned gas body in front is rapidly ignited and a large amount of energy is released. Then, the flame propagation velocity rises rapidly and reaches the second peak. Since then, due to the excessive stretching and mixing between hot and cold gases, the combustion rate and flame temperature decreases, which leads to the decrease of flame propagation velocity [22]. As the flame propagates to the open end, the pressure is relieved and thus the interference of the reflected waves to the flame front is reduced. Therefore, the propagation velocity increases gradually, reaching a maximum value of 500 m/s at the end of the pipe.

For the 90° elbow pipe structure, after the flame propagates to the first velocity peak with the fingertip structure, the area of flame front begins to decrease. The *flat* flame is formed at 2 m from the ignition end, where the flame propagation velocity decreases to the lowest. Then, the flame front reverses with shape changing from convex to concave and finally forms the *tulip flame* at 3 m, shown by the black dashed box, fig. 5(a). The special structure of the tulip flame increases the contact area between the flametip and the unburned gas, at the same time, the Kelvin-Helmholtz (K-H) instability of the flame is triggered by the velocity difference on the surface. The combined action of the special structure of flame and the K-H instability promote the secondary acceleration of flame to a certain extent. Later, when the flame passes through the elbow, the impact reflection near the concave wall forms a tongue-shaped flame, which accelerates the mixing of the flame and the unburned gas body and promotes combustion. The convex wall generates rarefaction waves, which reduces the rate of combustion chemical reaction [30]. Figure 7 shows that the deceleration effect produced by the convex wall plays a major role. It can be seen that the whole trend of flame propagation speed of the 90° elbow structure is similar to that of straight pipe, but the difference is that there is more turbulence generated in 90° elbow due to the shape change and the bend of pipe. Affected by the geometric shape of the 90° wall, the generated turbulence is a large-scale reverse companion flow, shown by the solid black box, fig. 5(a), which is generated from the formation of the *flat* flame and continues through the middle and later stages of combustion process. The reflected wave generated by the collision of reverse companion flow and high speed air-flow with the pipe wall leads to a partial flame extinction and energy reduction, causing the flame propagation velocity lower than that of the straight pipe. The maximum value is 357 m/s, which is 28.6% lower than that of the straight pipe.

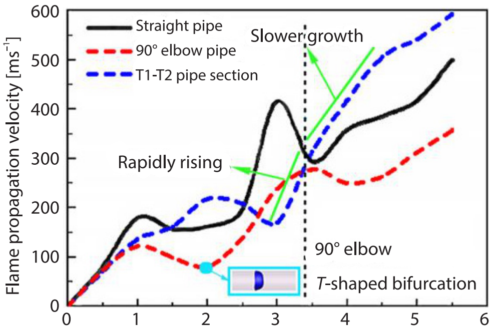

Figure 7. Flame propagation velocity diagram in each pipe structure

For the *T*-shaped bifurcation pipe structure, bifurcation is equivalent to a vent on the horizontal pipe section. When the flame propagates to the vent front (3 m from the ignition end), it will be pulled by the positive flow field, thus showing an acceleration effect. When the flame front passes through the explosion vent, there is a diversion, as shown in I, II, fig. 5(a).

Some flame enters the branch pipe and takes away some energy. Due to the combined effect of reflection wave and vertical flow field, the flame acceleration effect slows down and the rising rate decreases [31]. After that, the flame propagates to the pressure outlet, which is gradually accelerated by the effect of air-flow release. Finally, the flame velocity reaches the peak value of 592 m/s, which is 15.54% higher than that of straight pipe and 39.69% higher than that of 90° elbow.

The effect of different pipe-line structures on the explosion pressure

Figure 8 shows the pressure and pressure rise rate curve of each pipe structure under the end-opening conditions. The rate of pressure rise reflects the rising and falling process of pressure in the pipe. It can be seen that there are two peaks and two troughs in the pressure rise rate of each pipe structure, and the pressure change trend is basically the same, as shown in fig. 8. The superposition of pressure waves generated at the initial ignition stage forms compression waves, resulting in a rapid increase of pressure rise rate and an exponential increase of pressure. On one hand, the first inflection point of pressure is generated when the flame contacts the side wall of the pipe. The rapid reduction of the flame area leads to a rapid decrease of pressure rise rate. The inflection point of elbow pipe appears earlier than that of straight pipe, this is because the elbow structure pre-forms a relatively closed space, so a greater constraint leads to a higher pressure accumulation. [32, 33]. On the other hand, the sudden deceleration of the flame triggers a pressure wave [34]. As the pressure wave propagates to the right, the unburned region is occupied by positive flow, resulting in the accelerated propagation of the flame front and the second increase of pressure. In addition, the pressure wave is reflected when it encounters obstacles during propagation, and then propagates back and forth in the pipe-line. The oscillation of the corresponding section of the elbow pressure curve, shown by the green box, fig. (8) is closely related to this. Another significant inflection point of pressure occurs between 15 ms and 20 ms. At this time, the pressure increase is attributed to the increase of flame propagation velocity, and the inflection point of the elbow is still earlier than that of the straight pipe. This is because the bending structure affects the flame dynamics by promoting the growth of K-H and R-T instability [35]. The reflection effect generated by the elbow promotes the mixing of gas, and accelerates the combustion speed of the flame, and increases the superposition speed of the compression wave, leading to an increase in the rate of pressure rise. After that, the flame front becomes *flat* at about 20 ms, fig. 8(a), and the surface area reaches the minimum. Under the action of reverse companion flow, the propagation velocity decreases, the pressure rise rate decreases, so the pressure rises slowly, reaching the peak value of 0.059 MPa at about 23 ms. The formation of tulip flame at about 30 ms, fig. 8(b) causes the flame area to increase again and thus leads to the increase of pressure rise rate again.

In the *T*-shaped bifurcation pipe, when the shock wave enters the bifurcation, fig. 8(c), due to the sudden expansion of the cross-section and the rarefaction wave generated by the collision with the inflection Point A, as shown in fig. 8(c), part of the shock wave is extinguished, local diffraction occurs, and a *dead zone* is formed near Point A, shown in II, fig. 5(a). The wave front is bent, the explosion intensity is attenuated, and a large-scale turbulent vortex is formed in the *dead zone*, shown in III, fig. 5(a). Then the shock wave propagates forward to the inflection Point B, as shown in fig. 8(c), and the local flame is extinguished due to the influence of the rarefaction wave. The curved wave front has regular mirror reflection with the lower wall of the T2 branch pipe. The propagation of the reflected shock wave makes the flow field temperature rise again. As the reaction proceeds, the regular reflection of the shock wave gradually becomes Mach reflection [36]. After multiple reflections of the reflected shock wave between the wall surfaces of the T2 branch pipe, the unburned gas is heated and pressurized, resulting in a secondary ignition. The overpressure in the pipe rises rapidly to a peak value of 0.08 MPa.

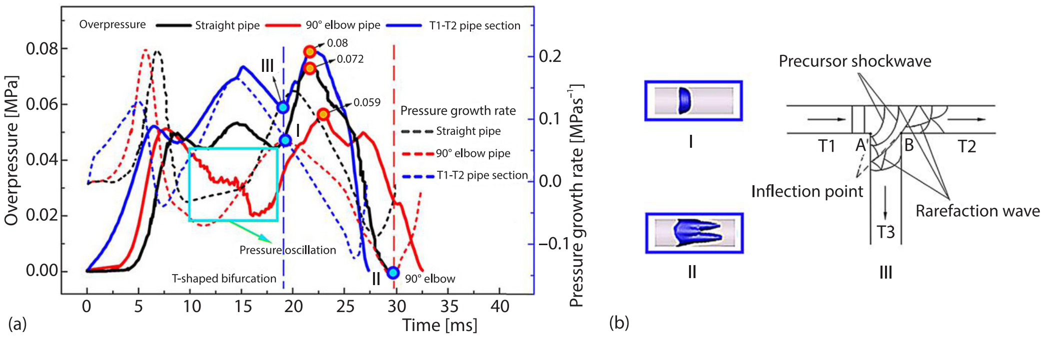

Figure 8. Effect of different pipe-line structures on the explosion pressure; (a) pressure curves and pressure rise rate curve in each pipe-line structure and (b) schematic diagram of flame structure and shock wave development at corresponding time of pipe-line marked on the curve

Conclusions

In this paper, based on the numerical simulation method, the combustion and explosion characteristics of hydrogen-air premixed gas in three pipe structures with open-end are studied, and the following conclusions are drawn. The conclusions reveal the flame propagation mechanism in the combustion process of hydrogen-air premixed gas, and provide some theoretical guidance for future pipe-line strength design, subsequent pipe-line safety check and accident mitigation, are as follows.

- In the end-opening pipe, the 90° elbow has a certain inhibitory effect on flame development. The maximum flame propagation velocity of 90° elbow is 357 m/s, which is 28.6% lower than that of straight pipe and 39.69% lower than that of *T*-shaped bifurcation pipe. The maximum explosion pressure is 0.059 MPa, which is 18.06% lower than that of straight pipe and 26.25% lower than that of *T*-shaped bifurcation pipe.
- In the end-opening pipe, the *T*-shaped bifurcation structure can effectively promote the combustion and explosion reaction. The maximum flame propagation velocity in the *T*-shaped bifurcation pipe is 592 m/s, which is 15.54% higher than that of the straight pipe and 39.69% higher than that of the 90° elbow. The maximum explosion pressure is 0.08 MPa, which is 10% higher than that of straight pipe and 26.25% higher than that of 90° elbow.
- Under the end-opening condition, there are two peaks and two troughs in the pressure rise rate curves of the three pipe structures, and the pressure change trend is basically the same. The air-flow release effect of the end-opening will greatly reduce the pressure in each pipe structure.

In the future research, the process of gas explosion in non-adiabatic wall pipes will be simulated. At present, the pipe wall is an adiabatic and non-slip wall. Although the duration of the explosion process is very short, so that the temperature has little influence on the load loading effect, in order to be more practical, the actual factors should be taken into account in the later simulation such as the heat dissipation of the pipe wall to further reduce the error.

Acknowledgment

This study was supported by the Innovative Talents Team Project of *Six Talents Peaks* in Jiangsu Province (No. Innovative Talents Team Project of *Six Talents Peaks* in Jiangsu Province Innovative Talents Team Project of *Six Talents Peaks* in Jiangsu Province TD-JNHB-013), Postgraduate Research and Practice Innovation Program of Jiangsu Province (SJCX22-1399), National Key R and D Program of China (No. 2017YFC0805100), Special Funding Project of Basic Scientific Research Business Fee of China Academy of Safety Production (No. 2019JBKY08), and Major Projects supported by the Natural Science Research of Jiangsu Higher Education Institutions (No. 17KJA440001).

Nomenclature

C – a scalar representing the reaction process, $C = 0$: reaction has not begun, $C = 1$: reaction is complete, [–]
$\tilde{c}$ – average reaction process variable, [–]
$|\nabla c|$ – gradient of the process variable, [–]
h_s – sensible enthalpy, [Pam^{-3}]
n – type of reactants, [–]
p – pressure, [Pa]
Sc_t – turbulent Schmidt number, [–]
S_t – turbulent flame velocity, [ms^{-1}]
t – time [s]
u – molecular viscosity, [Pa·s]
Y_i – mass fraction of component i, [–]
$Y_{i,e}$ – mass fraction of the component i during complete combustion, [–]

Greek symbols

λ – thermal conductivity, [Wm^{-1}K^{-1}]
ρ – density, [kgm^{-3}]
$\bar{\rho}_u$ – density of unburned gas, [kgm^{-3}]
τ_{ij} – subgrid-scale stress
Ξ_Δ – subgrid flame wrinkle coefficient, [–]

References

[1] Boukhelef, M., *et al*., Numerical Study of the Injection Conditions Effect on the Behavior of Hydrogen-Air Diffusion Flame, *Thermal Science*, *26* (2022), 5A, pp. 3741-3750
[2] Mintz, M., *et al*., Hydrogen: On the Horizon or Just a Mirage, *SAE Transactions*, *111* (2002), 4, pp. 911-921
[3] Chen, C. K., *et al*., Comparative Numerical Simulation Analysis on Explosion of Hydrogen and Propane in Highway Tunnel, *Journal of Safety Science and Technology*, *13* (2017), pp. 151-155
[4] Liu, Z. L., *et al*., Simulation Analysis on Leakage and Explosion Accident Consequence of Buried Hydrogen Pipe-Line, *Journal of Safety Science and Technology*, *15* (2019), pp. 94-100
[5] Yu, L. X., *et al*., Flame Propagation of H_2-air in a Semi-Open Obstructed Tube, *Journal of Combustion Science and Technology*, *8* (2002), 1, pp. 27-30
[6] Wen, X. J., *et al*., Numerical Study on Hydrogen Combustion in a Semiconfined Pipe with Obstacles, *Fire Safety Science*, *26* (2017), 2, pp. 61-67
[7] Uchida, M., *et al.*, Pressure Loading of Detonation Waves through 90-Degree Bend in High Pressure H_2-O_2-N_2 Mixtures, *Proceedings of the Combustion Institute*, *33* (2011), 2, pp. 2327-23332
[8] Li, M., *et al*., Experimental and Large Eddy Simulation Study on Gasoline-Air Mixture Explosions in Semi-Confined Pipe with 90° Right-Angle Bend, *CIESC Journal*, 69 (2018), 12, pp. 5370-5378
[9] Frolov, S. M., *et al*., Shock Wave and Detonation Propagation through U-Bend Tubes, *Proceedings of the Combustion Institute*, *31* (2007), 2, pp. 2421-2428
[10] [10] Zhou, N., *et al*., Effects of Ignition Position on Explosion of Premixed Propane-Air in a T-Type Pipe, *Process Safety Progress*, *40* (2020), 1, e12184
[11] Zhou, N., *et al*., Effect of Hydrogen Addition on the Explosion Characteristics of Methane-Hydrogen-Air Mixture in T-Shaped Bifurcation Pipe, Energy Sources – Part A: *Recovery, Utilization, and Environmental Effects*, *44* (2022), 2, pp. 3808-3822
[12] Zhou, N., *et al*., Experimental Study on Hydrogen-Air Premixed Gas Explosion in Confined Space, Energy Sources – Part A: *Recovery, Utilization, and Environmental Effects*, On-line first, https://doi.org/10.1080/15567036.2020.1782535, 2020
[13] Xiao, H. H., *et al*., An Experimental Study of Premixed Hydrogen/Air Flame Propagation in a Partially Open Duct, *International Journal of Hydrogen Energy*, *39* (2014), 11, pp. 6233-6241
[14] Ponizy, B., *et al*., Tulip flame – The Mechanism of Flame Front Inversion, *Combustion and Flame*, *161* (2014), 12, pp. 3051-3062

[15] Dostiyarov, A., *et al*., A Novel Vortex Combustion Device: Experiments and Numerical Simulations with Emphasis on the Combustion Process and NO_x Emissions, *Thermal Science*, *26* (2022), 2C, pp. 1971-1983
[16] Ciccarelli, G., Dorofeev, S., Flame Acceleration and Transition Detonation in Ducts, *Progress in Energy and Combustion Science*, *34* (2008), 4, pp. 499-550
[17] Xiao, H. H., *et al*., An Experimental Study of Distorted Tulip Flame Formation in a Closed Duct, *Combustion and Flame*, *160* (2013), 9, pp. 1725-1728
[18] Zhou, L. X., Basic Research and Numerical Simulation of Turbulent Two-Phase Combustion, *Combustion Science and Technology*, *19* (2013), 6, pp. 479-487
[19] Zhou, L. X., *et al*., Recent Research Progress of Large Eddy Simulation of Turbulent Combustion, *Journal of Engineering Thermophysics*, *27* (2006), 2, pp. 331-334
[20] Liu, Y., *et al*., Large Eddy Simulation and Its Application in Turbulent Combustion, *Advances in Mechanics*, *31* (2001), 2, pp. 215-226
[21] Lamoureux, N., *et al*., Laminar Flame Velocity Determination for H_2-air-He-CO_2 Mixtures Using the Spherical Bomb Method, *Experimental Thermal and Fluid Science*, *27* (2003), 4, pp. 385-393
[22] Lv, X. S., *et al*., Combined Effects of Obstacle Position and Equivalence Ratio on Overpressure of Premixed Hydrogen-Air Explosion, *International Journal of Hydrogen Energy*, *41* (2016), 39, pp. 17740-17749
[23] Chen, Y. Y., *et al*., The Misfire Degree and Its Effects on Combustion and Pollutant Formation of Subsequent Cycles: A Study on a High Speed Gasoline Engine, *Thermal Science*, *26* (2022), 2C, pp. 1649-1663
[24] Clanet, C., Searby, G., On the "Tulip Flame" Phenomenon, *Combustion and Flame*, *105* (1996), 1, pp. 225-238
[25] Matalon, M., Flame Dynamics, *Proceedings of the Combustion Institute*, *32* (2009), 1, pp. 57-82
[26] Bychkov, V. V., Liberman, M. A., Dynamics and Stability of Premixed Flames, *Physics Reports*, *325* (2000), 4, pp. 116-237
[27] Mei, Y., *et al*., Flame Propagation of Premixed Hydrogen-Air Explosions in Bend Pipes, *Journal of Loss Prevention in the Process Industries*, *77* (2022), July, 104790
[28] Zhu, Y. J., *et al*., A Numerical Study on Shock Induced Distortion, Mixing and Combustion of Flame, *Explosion and Shock Waves*, *33* (2013), 4, pp. 430-437
[29] Zhou, N., *et al*., Numerical Simulation of the Influence of Vent Conditions on H_2/air Explosion Characteristics, *Chemical Industry and Engineering Progress*, *40* (2021), 4, pp. 3656-3663
[30] Zhou, N., *et al*., Numerical Simulation Study on the Combustion Rule of Bending Structure in Pipes, *Combustion Science and Technology*, *190* (2018), 9, pp. 1500-1514
[31] Sun, H., *et al*., Numerical Simulation of the Influence of Vent on Hydrogen Flame Propagation in Pipeline, *Industrial Safety and Environmental Protection*, *47* (2021), 12, pp. 7-11
[32] Blanchard, R., *et al*., Explosions in Closed Pipes Containing Baffles and 90 Degree Bends, *Journal of Loss Prevention in the Process Industries*, *23* (2010), 2, pp. 253-259
[33] Ugarte, O. J., *et al*., Critical Role of Blockage Ratio for Flame Acceleration in Channels with Tightly Spaced Obstacles, *Physics of Fluids*, *28* (2016), 9, 093602
[34] Gonzalez, M., Acoustic Instability of a Premixed Flame Propagating in a Tube, *Combustion and Flame*, *107* (1996), 3, pp. 245-259
[35] Xiao, H. H., *et al*., A Study on the Dynamic Behavior of Premixed Propane-Air Flames Propagating in a Curved Combustion Chamber, *Fuel*, 228 (2018), Sept., pp. 342-348
[36] Wang, C. J., *et al*., Gaseous Detonation Propagation in a Bifurcated Tube, *Journal of Fluid Mechanics*, *599* (2008), Mar., pp. 81-110

Paper submitted: September 10, 2022
Paper revised: October 15, 2022
Paper accepted: October 18, 2022